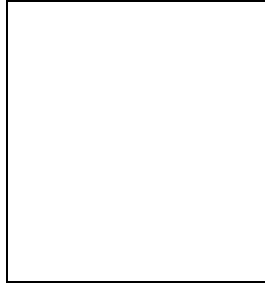


RUNNING OF THE QED COUPLING IN SMALL-ANGLE BHABHA  
SCATTERING AT LEP

G. ABBIENDI

INFN and Dipartimento di Fisica dell'Università di Bologna, Viale C. Berti-Pichat 6/2,  
40127 Bologna, Italy



Using the OPAL detector at LEP, the running of the effective QED coupling  $\alpha(t)$  is measured for space-like momentum transfer,  $2 < t < 6 \text{ GeV}^2$ , from the angular distribution of small-angle Bhabha scattering. This is currently the most significant direct observation of the running of the QED coupling in a single experiment and the first clear evidence of the hadronic contribution to the running in the space-like region. Our result is in good agreement with standard evaluations of  $\alpha(t)$ , based on data in the time-like region.

## 1 Introduction

The effective QED coupling  $\alpha(t)$  is an essential ingredient for many precision physics predictions. It contributes one of the dominant uncertainties in the electroweak fits constraining the Higgs mass. The effective QED coupling is generally expressed as:

$$\alpha(t) = \frac{\alpha_0}{1 - \Pi(t)} \quad (1)$$

where  $\alpha_0 = \alpha(t=0)$ ,  $1/137$  is the fine structure constant,  $t$  is the momentum transfer squared of the exchanged photon and  $\Pi$  is the vacuum polarization contribution. Whereas the leptonic contributions to  $\Pi$  are calculable to very high accuracy, the hadronic ones have to be evaluated by using a dispersion integral over the measured cross section of  $e^+e^- \rightarrow \text{hadrons}$  at low energies, plus perturbative QCD<sup>1;2</sup>. There are also many evaluations which are more theory-driven, extending the application of perturbative QCD down to  $\sqrt{2} \text{ GeV}$  (see for example the reference<sup>3</sup>). An alternative approach<sup>4</sup> uses perturbative QCD in the negative  $t$  (space-like) region.

There have been only a few direct observations of the running of the QED coupling<sup>5;6;7;8</sup>. Here we present a new result from the OPAL collaboration. A full description can be found

in the OPAL paper<sup>9</sup>. The running of  $\alpha$  is measured in the space-like region, by studying the angular dependence of small-angle Bhabha scattering,  $e^+e^- \rightarrow e^+e^-$ , at LEP. Small-angle Bhabha scattering appears to be an ideal process for a direct measurement of the running of  $\alpha(t)$  in a single experiment, as it is an almost pure QED process, strongly dominated by t-channel photon exchange. Moreover the data sample has large statistics and excellent purity. The Bhabha differential cross section can be written in the following form for small scattering angle:

$$\frac{d}{dt} = \frac{d^{(0)}}{dt} - \frac{\delta(t)}{t^2} (1 + \delta) (1 + \delta) + \delta_Z \quad (2)$$

where  $d^{(0)}/dt = 4\pi\alpha^2/t^2$  is the Born term for the t-channel diagram,  $\delta$  represents the radiative corrections to the Born cross section, while  $\delta$  and  $\delta_Z$  are the interference contributions with s-channel photon and Z exchange respectively.  $\delta$  and  $\delta_Z$  are much smaller than  $\delta$  and the vacuum polarization. Therefore, with a precise knowledge of the radiative corrections ( $\delta$  term) one can determine the effective coupling  $\alpha(t)$  by measuring the differential cross section. This method has also been advocated in a recent paper<sup>10</sup>.

## 2 Detector and event selection

We use OPAL data collected in 1993–95 at energies close to the Z resonance peak. In particular this analysis is based on the OPAL SiW calorimeter<sup>11</sup>. The SiW consisted of two cylindrical calorimeters encircling the beam pipe at a distance  $z' = 2.5$  m from the interaction point. Each calorimeter was a stack of 19 silicon layers interleaved with 18 tungsten plates, with a sensitive depth of 14 cm, representing 22 radiation lengths ( $X_0$ ). The sensitive area fully covered radii between 6.2 and 14.2 cm from the beam axis, corresponding to scattering angles between 25 and 58 mrad. Each detector layer was segmented with R-geometry in a  $32 \times 32$  pad array. The pad size was 2.5 mm radially and 11.25 degrees in azimuth. In total the whole calorimeter had 38,912 readout channels corresponding to the individual silicon pads. Particles coming from the interaction point had to traverse the material constituting the beam pipe and its support structures as well as detector cables before reaching the face of the SiW calorimeters. This preshowering material was minimum near the inner angular limit, about  $0.25X_0$ , while in the middle of the acceptance it increased to about  $2X_0$ . When LEP 2 data-taking started in 1996 the detector configuration changed, with the installation of tungsten shields designed to protect the inner tracking detectors from synchrotron radiation. This reduced the useful acceptance of the detector at the lower angular limit. Therefore we limited this analysis to the LEP 1 data.

The event selection is similar to the one used for luminosity measurements<sup>11</sup>. The selected sample is strongly dominated by two-cluster configurations, with almost full energy back-to-back  $e^+$  and  $e^-$  incident on the two calorimeters. At leading order the momentum transfer squared  $t$  is simply related to the scattering angle  $\theta$ , which is measured from the radial position  $R$  of the scattered  $e^+$  and  $e^-$  at reference planes located within the SiW calorimeters:

$$t = s \frac{1 - \cos\theta}{2} = \frac{s^2}{4}; \quad \tan\theta = R/z \quad (3)$$

At the center-of-mass energy  $\sqrt{s} = 91$  GeV our angular acceptance corresponds to  $2 < \theta < 6$  GeV<sup>2</sup>.

The radial distributions are shown in Fig. 1 for the complete data statistics, compared to the Monte Carlo distributions normalized to the same number of events. Due to the back-to-back nature of Bhabha events, the two sides do not contribute independent statistical information. After the studies mentioned in section 4, we decided to use the Right side distribution for the analyses, to keep at minimum possible unassessed systematic errors. Consistent results are obtained with the use of the Left side distribution.

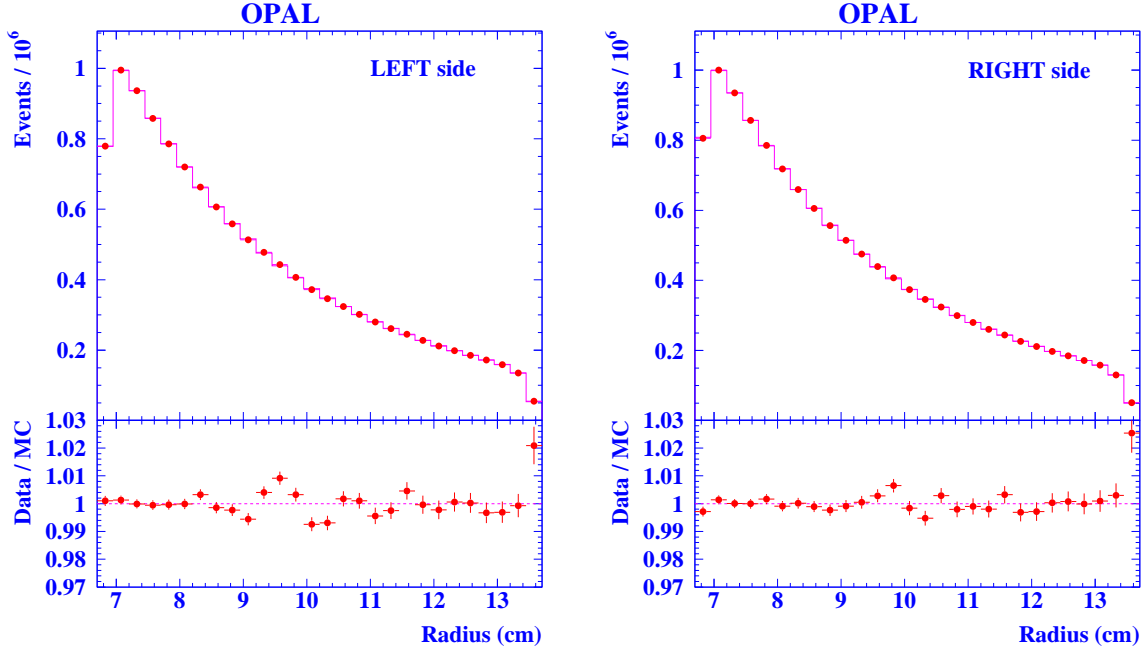


Figure 1: Radial distributions for the complete data statistics. The points show the data and the histogram the Monte Carlo prediction, assuming the expected running of  $\alpha$ , normalized to the same number of events. The lower plots show the ratio between data and Monte Carlo.

### 3 Fit method

The counting rate of Bhabha events in the SW is used to determine the integrated luminosity, so that we cannot make an absolute measurement of  $\sigma(t)$  without an independent determination of the luminosity.

We compare the radial distribution of the data (and hence the  $t$ -spectrum) with the predictions of the BHLUMI Monte Carlo<sup>12</sup>. This is a multiphoton exponentiated generator accurate up to the leading logarithmic  $O(L^2)$  terms<sup>a</sup>. Higher order photonic contributions are partially included by virtue of the exponentiation. It has been used to determine the luminosity at LEP and has been widely cross-checked with many alternative calculations. If the Monte Carlo is modified by setting the coupling to the constant value  $\alpha(t) = \alpha_0$ , the ratio  $f$  of the number of data to Monte Carlo events in a given radial bin is:

$$f(t) = \frac{N_{\text{data}}(t)}{N_{\text{MC}}^0(t)} / \frac{1}{1 - \alpha(t)}^2 \quad (4)$$

The dominant dependence of  $\alpha(t)$  expected from theory is logarithmic. We therefore fitted the ratio  $f(t)$  as:

$$f(t) = a + b \ln \frac{t}{t_0} \quad (5)$$

where  $t_0 = 3.3 \text{ GeV}^2$  is the mean value of  $t$  in the data sample. The parameter  $a$ , about unity, is not relevant since the Monte Carlo is normalized to the data. The slope  $b$  represents the full observable effect of the running of  $\alpha(t)$ , both the leptonic and hadronic components. It is related to the variation of the coupling by:

$$\alpha(t_2) - \alpha(t_1) = \frac{b}{2} \ln \frac{t_2}{t_1} \quad (6)$$

<sup>a</sup> $L = \ln(\frac{t}{m_e^2})$  is the large logarithm.

Table 1: Fit result for each dataset and average. For each value of  $b$  the first error is statistical and the second the full experimental systematic.

Dataset	$\bar{p}_s$ (GeV)	Number of events	slope $b$ ( $10^{-5}$ )		
93-2	89.4510	879549	662	326	89
93-pk	91.2228	894206	670	324	92
93+2	93.0362	852106	640	332	89
94-a	91.2354	885606	559	326	86
94-b	91.2170	4069876	936	152	71
94-c	91.2436	288813	62	570	122
95-2	89.4416	890248	839	325	124
95-pk	91.2860	581111	727	402	126
95+2	92.9720	885837	156	325	128
Average	91.2208	10227352	726	96	70
$\chi^2$ =d.o.f. (stat.)			6:9=8		
$\chi^2$ =d.o.f. (stat.+ syst.)			6:5=8		

where  $t_1 = 1.81 \text{ GeV}^2$  and  $t_2 = 6.07 \text{ GeV}^2$  correspond to the acceptance limits.

#### 4 Main systematic effects

It is important to realize which systematic effects could mimic the expected running or disturb the measurement. The most potentially harmful effects are biases in the reconstructed radial coordinate. Most simply one could think of dividing the detector acceptance into two and determining the slope using only two bins. In such a model the running is equivalent to a bias in the central division of  $70 \text{ m}$ . Biases on the inner or outer radial cut have a little less importance and could mimic the full running for  $90$  or  $210 \text{ m}$  systematic offsets respectively. Concerning radial metrology, a uniform bias of  $0.5 \text{ mm}$  on all radii would give the same observable slope as the expected running. Knowledge of the beam parameters, particularly the transverse offset and the beam divergence, is also quite important. Thus, limitation of systematic error in the reconstructed radial coordinate is key to the current measurement.

Details of how the coordinates are formed from the recorded pad information are found in [11](#). The fine radial and longitudinal granularity of the detector are exploited to produce precise radial coordinates. The reconstruction determines the radial coordinate of the highest energy cluster, in each of the Right and Left calorimeters. Each coordinate uses a large number of pads throughout the detector, from many silicon layers, and is projected onto a reference layer, close to the average longitudinal shower maximum. The residual bias, or anchor, of this radial coordinate is then estimated at each pad boundary in a given layer of the detector. Here we rely on the fact that, on average, the pad with the maximum signal in any particular layer will contain the shower axis. Then from the anchors we obtain bin-by-bin acceptance corrections which are applied to the radial distribution. This procedure, named anchoring, is the most delicate part of the analysis, and was carefully studied [9](#). The challenging aspect is controlling the residual bias on the radial coordinate to a level below  $10 \text{ m}$  uniformly throughout the acceptance.

#### 5 Results

The ratio of data to Monte Carlo is fitted to Eq. 5 and the results are given in Table 1. The

## OPAL

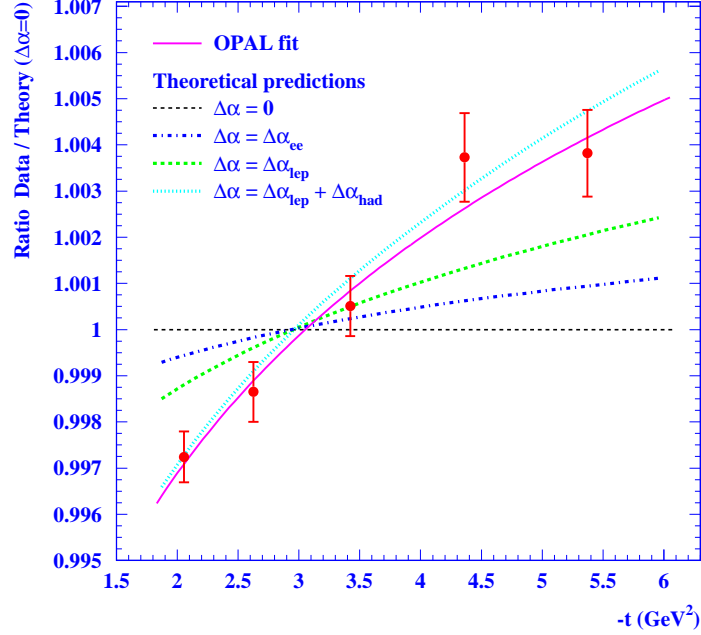


Figure 2:  $\mu\mu$  spectrum normalized to the BHLUM I theoretical prediction for a fixed coupling ( $\Delta\alpha = 0$ ). The points show the combined OPAL data with statistical error bars. The solid line is our fit. The horizontal line (Ratio=1) is the prediction if  $\alpha$  were fixed. The dot-dashed curve is the prediction of running determined by vacuum polarization with only virtual  $e^+e^-$  pairs, the dashed curve includes all charged lepton pairs and the dotted curve the full Standard Model prediction, with both lepton and quark pairs.

nine datasets give consistent results, with  $\chi^2/\text{d.o.f} = 6.9/8$  for the average  $b$  considering only statistical errors. The most important systematic errors come from the anchoring procedure and the preshowering material, both affecting the radial coordinate. The fit results are then combined, by considering the full error correlation matrix, obtaining:

$$b = (726 \quad 96 \quad 70 \quad 50) \cdot 10^{-5}$$

where here, and also in the results quoted below, the first error is statistical, the second is the experimental systematic and the third is the theoretical uncertainty. The total significance of the measurement is 5.6  $\sigma$ .

The theoretical uncertainty is dominated by the photonic corrections to the leading  $t$ -channel diagram, in particular by missing  $\mathcal{O}(\alpha^2 L)$  terms, and the technical precision of the calculation. We estimated these uncertainties by comparing BHLUM I with alternative Monte Carlo calculations. Other uncertainties, from  $Z$  interference and the contribution of light  $e^+e^-$  pairs, were also estimated and added in quadrature.

The result for the combined data sample is illustrated in Fig. 2. The logarithmic fit to Eq. 5 describes the data very well,  $\chi^2/\text{d.o.f} = 1.9/3$ , although a simple linear fit would also be adequate, giving  $\chi^2/\text{d.o.f} = 2.7/3$ . The data are clearly incompatible with the hypothesis of a fixed coupling. The fitted logarithmic dependence agrees well with the full Standard Model prediction including both leptonic and hadronic contributions, with the hadronic part obtained by the Burkhardt-Pietrzyk parameterization<sup>2</sup>. Our result can be easily compared to the previous one by L3<sup>8</sup>. If the latter is expressed as a slope according to Eq. 6, it becomes:  $b^{(L3)} = (1044 \quad 348) \cdot 10^{-5}$ , with a larger error dominated by experimental systematics but consistent with ours.

The effective slope gives a measurement of the variation of the coupling  $\alpha(t)$  from Eq. 6:

$$\alpha(6.07 \text{ GeV}^2) - \alpha(1.81 \text{ GeV}^2) = (440 \pm 58 \pm 43 \pm 30) \cdot 10^{-5} :$$

This is in good agreement with the Standard Model prediction, which gives  $\alpha(t) = (460 \pm 16) \cdot 10^{-5}$  for the same  $t$  interval, where the error originates from the uncertainty of the hadronic component. The evaluation  $\alpha_{\text{had}}^2$  of  $\alpha_{\text{had}}$  has a relative precision ranging from 2.5% at  $t = 1.81 \text{ GeV}^2$  to 2.7% at  $t = 6.07 \text{ GeV}^2$  [13].

The absolute value of  $\alpha$  in our range of  $t$  is expected to be dominated by  $e^+e^-$  pairs, with the relevant fermion species contributing in the approximate proportions:  $e^+e^- : \text{hadron} \approx 4 : 1 : 2$ . Our measurement is sensitive, however, not to the absolute value of  $\alpha$ , but only to its slope within our  $t$  range. Contributions to the slope in this range are predicted to be in the proportion:  $e^+e^- : \text{hadron} \approx 1 : 1 : 2.5$ . Fig. 2 shows these expectations graphically. We can discard the hypothesis of running due only to virtual  $e^+e^-$  pairs with a significance of 4:1.

The data are also incompatible with the hypothesis of running due only to leptons. If we subtract the precisely calculable theoretical prediction for all leptonic contributions,  $\alpha_{\text{lep}} = 202 \cdot 10^{-5}$ , from the measured result, we can determine the hadronic contribution as:

$$\alpha_{\text{had}}(6.07 \text{ GeV}^2) - \alpha_{\text{had}}(1.81 \text{ GeV}^2) = (237 \pm 58 \pm 43 \pm 30) \cdot 10^{-5} :$$

This has a significance of 3.0, considering all the errors.

## 6 Conclusions

We have measured the scale dependence of the effective QED coupling from the angular distribution of small-angle Bhabha scattering at LEP, using the precise OPAL Silicon-Tungsten luminometer. We obtain the strongest direct evidence for the running of the QED coupling ever achieved in a single experiment, with a significance above 5. Moreover we report the first clear experimental evidence for the hadronic contribution to the running in the space-like region, with a significance of 3. This measurement is one of only a very few experimental tests of the running of  $\alpha(t)$  in the space-like region, where  $\alpha$  has a smooth behaviour. Our result is in good agreement with standard evaluations of  $\alpha(t)$ , based on data in the time-like region.

## References

1. S. Eidelman and F. Jegerlehner, *Z. Phys. C* 67, 585 (1995).
2. H. Burkhardt and B. Pietrzyk, *Phys. Lett. B* 513, 46 (2001).
3. J. F. de Troconiz and F. J. Yndurain, *Phys. Rev. D* 71, 073008 (2005).
4. S. Eidelman, et al., *Phys. Lett. B* 454, 369 (1999); F. Jegerlehner, hep-ph/0308117.
5. TOPAZ Collaboration, I. Levine et al., *Phys. Rev. Lett.* 78, 424 (1997).
6. OPAL Collaboration, G. Abbiendi et al., *Eur. Phys. J. C* 33, 173 (2004).
7. VENUS Collaboration, S. Otake et al., *Phys. Rev. Lett.* 81, 2428 (1998).
8. L3 Collaboration, M. Acciarri et al., *Phys. Lett. B* 476, 40 (2000).
9. OPAL Collaboration, G. Abbiendi et al., submitted to *Eur. Phys. J. C*, <http://opalinfo.cern.ch/opal/doc/paper/info/pr407.html>.
10. A. B. Arbuzov et al., *Eur. Phys. J. C* 34, 267 (2004).
11. OPAL Collaboration, G. Abbiendi et al., *Eur. Phys. J. C* 14, 373 (2000).
12. S. Jadach et al., *Comput. Phys. Commun.* 102, 229 (1997).
13. H. Burkhardt and B. Pietrzyk, private communication.